Published online 14 March 2012

Nucleic Acids Research, 2012, Vol. 40, No. 12 ***e88***
doi:10.1093/nar/gks232

Real-time assay for testing components of protein synthesis

Gabriel Rosenblum[1,2], Chunlai Chen[2], Jaskiran Kaur[3], Xiaonan Cui[2], Yale E. Goldman[2,*] and Barry S. Cooperman[1,*]

[1]The Department of Chemistry, University of Pennsylvania, 231 South 34th Street, [2]Pennsylvania Muscle Institute, University of Pennsylvania, 3700 Hamilton Walk-D700 Richards Building, Philadelphia, Pennsylvania 19104 and [3]Anima Cell Metrology 75 Claremont Road, Suite 102, Bernardsville, NJ 07924-2270, USA

Received November 16, 2011; Revised February 26, 2012; Accepted February 27, 2012

ABSTRACT

We present a flexible, real-time-coupled transcription–translation assay that involves the continuous monitoring of fluorescent Emerald GFP formation. Along with numerical simulation of a reaction kinetics model, the assay permits quantitative estimation of the effects on full-length protein synthesis of various additions, subtractions or substitutions to the protein synthesis machinery. Since the assay uses continuous fluorescence monitoring, it is much simpler and more rapid than other assays of protein synthesis and is compatible with high-throughput formats. Straightforward alterations of the assay permit determination of (i) the fraction of ribosomes in a cell-free protein synthesis kit that is active in full-length protein synthesis and (ii) the relative activities in supporting protein synthesis of modified (e.g. mutated, fluorescent-labeled) exogenous components (ribosomes, amino acid-specific tRNAs) that replace the corresponding endogenous components. Ribosomes containing fluorescent-labeled L11 and tRNAs labeled with fluorophores in the D-loop retain substantial activity. In the latter case, the extent of activity loss correlates with a combination of steric bulk and hydrophobicity of the fluorophore.

INTRODUCTION

Protein synthesis is being studied intensively with a variety of motivations, ranging from practical needs for the development of efficient methods of cell-free protein synthesis (CFPS) for production of proteins that are difficult to express in cells (1–3), for the identification of new antibiotics (4,5), and toward achieving understanding of basic mechanisms of individual steps of the translation cycle and of overall protein synthesis (6,7). Many mechanistic studies employ fluorescent-labeled constituents of the protein synthesis machinery. Fluorescent probes permit real-time monitoring of specific reaction steps (8–15), but raise the question of whether introduction of exogenous labels unduly affects the processes under study. Assays of protein synthesis in current use are often cumbersome, involving aliquot removal and subsequent point-by-point determinations of bioluminescence (3), fluorescence (16,17), gel densitometry (16), enzymatic activity assay (18,19) or incorporation of radioactive amino acids (20–22).

Here we present a flexible, real-time coupled transcription–translation assay that, along with numerical simulation of a reaction kinetics model, permits quantitative estimation of the effects on full-length protein synthesis of introducing fluorescent probes, or other modifications, into components of the translational machinery. The assay involves the continuous monitoring of the formation of Emerald GFP (EmGFP), a rapidly maturing variant of green fluorescent protein (23), using a suitable plasmid and a commercially available CFPS kit derived from *Escherichia coli* (24). Straightforward alterations of the assay permit determination of (i) the fraction of ribosomes in a cell-free protein synthesis kit that is active in full-length protein synthesis and (ii) the relative activities in supporting protein synthesis of modified (e.g. mutated, fluorescent-labeled) exogenous components (ribosomes, amino acid-specific tRNAs) that replace the corresponding endogenous components.

Since the assay uses continuous fluorescence monitoring, it is much simpler and more rapid to use than other assays of protein synthesis and is compatible with high-throughput formats. It should thus find widespread application in many studies measuring protein synthesis *in vitro*. However, the assay does have the significant limitation that it is extremely stringent, since it treats as fully

*To whom correspondence should be addressed. Email: goldmany@mail.med.upenn.edu
Correspondence may also be addressed to Barry S. Cooperman. Tel: +1 215 898 6330; Email: cooprman@pobox.upenn.edu

inactive those ribosomes that produce only partial or otherwise non-fluorescent EmGFP polypeptides.

MATERIALS AND METHODS

All solutions contained water of high purity generated by MilliQ deionizer equipped with pyrogen free filter (Biopak, Millipore) to ensure the absence of contaminating RNAses, DNAses and proteases. All ultracentrifugations at 110 000 r.p.m. were carried out in a S120AT2 rotor in a Sorvall M120SE ultracentrifuge. Ribosome concentrations were calculated assuming 26 pmol/A_{260} (25).

Exogenous component preparation

Plasmid

The pREST-EmGFP plasmid (Invitrogen, Inc.) contains a reading frame that includes a 40-residue N-terminal His-tag sequence followed by the 239-residue EmGFP sequence. We used standard mutagenesis techniques to introduce two modifications. The first, following reference (26), was to add a 31-residue C-terminal segment ending with the HindIII restriction site that, following plasmid linearization with HindIII, resulted in a reading frame devoid of a stop codon. This allowed tethering of mature, nascent EmGFPs to the ribosomes. The second change was a point mutation (S4F) near the beginning of the N-terminal His-tag sequence that was introduced for use in other studies. Mutagenesis was performed using a QuikChange Lightning site-directed mutagenesis kit (Stratagene, Inc.) with primers set according to the manufacturer's instructions.

Ribosomes

All preparative steps were carried out on ice or at 4°C. S30 fractions of *E. coli* strains MRE600 (wild type) and AM77 (−L11) were prepared as previously described (27) using a French Press at 5000 psi. Crude ribosome pellets were prepared by centrifuging S30 fractions at 110 000 rpm for 12 min at 4°C either directly (S100P), or by layering the S30 lysate on a sucrose cushion (S100sucP, using 1.1 M sucrose in TAM_{15} buffer) followed by resuspending the resulting pellet in TAM_{15} buffer. Small scale ribosome purification (70S-ss) was achieved by layering S100sucP ribosomes on a linear 15–30% sucrose gradient and collecting the 70S peak as described, using a VTi50 rotor (28). Large-scale ribosome purification (70S-ls) was achieved by sucrose gradient centrifugation using a zonal rotor as described (9). S100P preparations of $AM77^{L11}$or $AM77^{L11Cy3}$ ribosomes were prepared by incubating AM77 S30 fractions with a 2-fold excess of either unlabeled C38S/S87C-L11 (L11) or Cy3-labeled C38S/S87C-L11 ($L11^{Cy3}$) at 37°C for 15 min prior to high-speed pelleting. The preparation of the L11 variant and its labeling by Cy3 is described in (11). FPLC-purified $L11^{Cy3}$ contained 1.0 Cy3/protein.

tRNA

The charging and fluorescent labeling of yeast and *E. coli* $tRNA^{Phe}$s (Chemical Block, Moscow) were performed as previously described (10,11). tRNA concentrations were calculated on the basis of the amount of charged material, as determined by ^{14}C-Phe radioactivity.

In vitro protein synthesis of EmGFP

Using the cell-free protein synthesis kit

The CFPS kit (RTS 100 *E. coli* HY kit – previously sold by Roche Applied Science, currently sold by 5prime) was utilized to synthesize EmGFP according to the manufacturer's manual, with some modifications. The CFPS kit is made up of five vials, containing cell lysate (V1), reaction mixture (V2), 19 amino acids (V3), methionine (V4), reconstitution buffer (V5) and a control GFP vector that was substituted throughout these experiments with the modified pREST-EmGFP plasmid described above. In the standard reaction, the following components are pre-mixed on ice: 2.4 µl V1, 2 µl V2, 2.4 µl V3, 0.2 µl V4, 1 µl V5 and 2 µl (130 ng) plasmid in water. The total reaction volume was ~10 µl. Fluorescence is recorded continuously at 30°C. The V3 solution was sometimes substituted by a home-made solution that contained approximately twice the original amino acid concentrations (denoted V3a). V3a, made up in V5, contained 8.33 mM tyrosine, 16.66 mM of each of the 18 other amino acids and no methionine. Final amino acid concentrations in the CFPS mixture were: 10 mM Met, 1 mM Tyr and 2 mM of the other amino acids. All other lyophilized CFPS components, were dissolved in V5 according to the manufacturer's manual, flash-frozen and stored at −80°C in single-use aliquots.

To test the activity of various buffers (Figure 1A) the following components were mixed: 2.4 µl V1, 2 µl V2, 1.2 µl V3a, 0.2 µl V4, 9.2 µl of the indicated buffer and 0.45 µl plasmid (stock solution 430 ng/µl in water). V3a was made up in the indicated buffer rather than in V5. The total volume of the reaction was ~15 µl. This combination yielded a reaction mixture that contained at least 70% of the indicated test buffer by volume and 30% of V5 used to reconstitute the lyophilized V1, V2 and V4. The buffers tested, included: TAM_{15}: 50 mM Tris–HCl pH 7.5, 30 mM NH_4Cl, 70 mM KCl, 15 mM $Mg(Ac)_2$, 1 mM DTT; TAM_7: 50 mM Tris–HCl pH 7.5, 70 mM NH_4Cl, 30 mM KCl, 7 mM $MgCl_2$, 1 mM DTT (29); Polymix Buffer: 50 mM Tris–HAc pH 7.5, 5 mM NH_4Ac,100 mM KCl, 15 mM $Mg(Ac)_2$, 0.5 mM $Ca(Ac)_2$, 6 mM 2-mercaptoethanol, 5 mM putrescine and 1 mM spermidine (30); Polyamine Buffer: 20 mM HEPES–KOH pH 7.5, 150 mM NH_4Ac, 4.5 mM $MgAc_2$, 4 mM 2-mercaptoethanol, 0.05 mM spermine and 2 mM spermidine (31).

Using the CFPS$^{-ribosome}$ kit

Ribosomes were removed from a mixture containing 2.4 µl V1, 2 µl V2, 1.2 µl V3 and 0.2 µl V4 as the pellet formed by ultracentrifugation at 110,000 rpm for 12 min at 4°C to yield the $CFPS^{-ribosome}$ kit. EmGFP synthesis was accomplished by adding 2.2 µl of 6.8 µM stock solution of home-made ribosomes (see above) in TAM_{15} buffer to the kit and initiating reaction with 130 ng of plasmid in 2 µl water. The final ribosome concentration of 1.5 µM equals the concentration found in the CFPS kit.

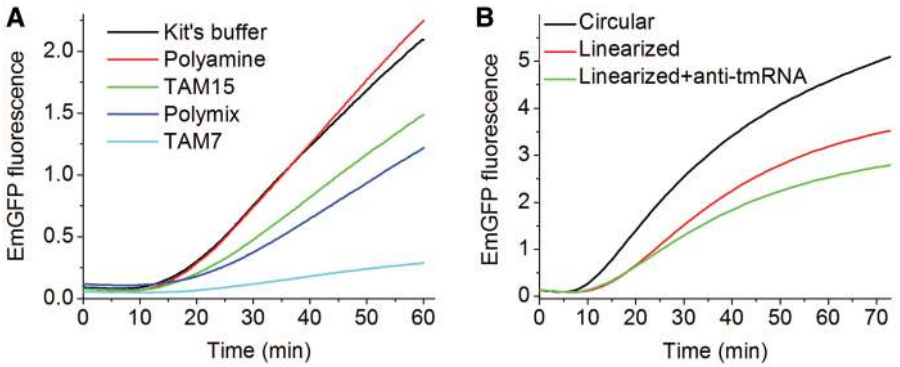

Figure 1. Cell-free expression of EmGFP using the CFPS kit. (**A**) Buffer dependence. Activity was determined using the indicated buffers. The reaction volumes were diluted (dilution factor of 1.5) to 15 µl and measured in the fluorometer every 20 s. (**B**) Plasmid dependence. Activity was determined, using the buffer provided with the kit for the indicated plasmids. Anti-tmRNA oligo DNA at a concentration of 5 µM was added in addition to the linearized plasmid to prevent dissociation of the ribosome-EmGFP complex. All experiments were preformed in triplicate. Signal was acquired every 45 s, avoiding sample irradiation between consecutive measurements in order to minimize photobleaching.

Using the CFPS^{-Phe} kit

Construction of the CFPS^{-Phe} kit required treatment of various solutions with an inhibition cocktail [100 µl of a commercial mixture of protease inhibitors (Halt, Pierce) and 0.5 µl of 4.7 M *N*-benzyl-2-phenylethylamine (Acros), a Phe-RS inhibitor (32)] and preparation of a V3a solution lacking Phe (denoted V3a-Phe). Additional details are found in Supplementary Information 2C and Supplementary Figure S3C. In addition, the normal ribosome concentration was sometimes reduced by half.

V1 (24 µl) was combined with 0.24 µl of an inhibition cocktail and the resulting mixture was dialyzed against 40 ml of TAM_{15} buffer supplemented with 5% PEG-8000 (Fisher) in 3.5 kDa cutoff micro-dialysis cups (Slide-A-Lyzer, Pierce—soaked in water for 15 min prior to first use). Following dialysis at 4°C for 30 min, 0.24 µl of fresh inhibition cocktail was added and dialysis was repeated against fresh buffer. The dialyzed V1 solution (24 µl) was combined with 20 µl V2, 12 µl V3a–Phe, 2 µl V4, 0.24 µl inhibition cocktail and 0.42 µl 10× of Polyamine buffer, generating the CFPS^{-Phe} solution. Reduction of ribosome concentration was accomplished by combining equal volumes of a ribosome-containing CFPS^{-Phe} kit and a ribosome-depleted CFPS^{-Phe} kit, prepared via high-speed centrifugation as described above.

EmGFP synthesis was accomplished by adding aqueous solutions (3.8 µl) of various concentrations of Phe-tRNA^{Phe} or Phe to the CFPS^{-Phe} kit (6.2 µl), followed by incubating the resulting mixture at 37°C for 5 min to promote ternary complex (EF-Tu•aa-tRNA•GTP) formation, and initiating the reaction with 130 ng plasmid in water (0.3 µl). Addition of EF-Tu in amounts equimolar with added Phe-tRNA^{Phe} results in a loss of EmGFP production (Supplementary Information 2F and Supplementary Figure S3F).

Other methods

Real-time fluorescence detection

Assays were performed at 30°C. Most assays were carried out in triplicates on a reaction volume of 10 µl dispensed in 384 well-plates (Greiner Bio-One 784076). Readings were taken every 20–45 s for 30–70 min in a plate reader (Envision 2103, Perkin-Elmer). The exposure time for individual fluorescence determinations was ~30 ms using 10 flashes/measurement. In the absence of dye-labeled exogenous components, filters/bandpass settings of λ_{ex} = 486/10 nm, λ_{em} = 535/25 nm were employed. To overcome spectral overlap of EmGFP emission with Cy3 and/or Cy5, the optimal settings were found to be λ_{ex} = 450/8 nm, λ_{em} = 510/10 nm (see Supplementary Information 3 and Supplementary Figure S5). Some assays were also carried out using a reaction volume of 15 µl placed in a sub-micro fluorometer cell (Starna Cells, Inc) placed within a spectrofluorometer (Hobira Jobin Yvon) (λ_{ex} = 468 nm, λ_{em} = 510 nm). Kinetic traces were recorded over 30 min at 10 s intervals, using a 1 s integration time.

EmGFP displays a fast component of photobleaching (33). To minimize photobleaching, sample irradiation was avoided except during recording, both in the fluorometer and in the plate reader. In a control experiment, no appreciable loss in EmGFP fluorescence could be detected over 70 min for purified EmGFP added to a CFPS^{-Phe} kit using the employed plate reader configuration, although photobleaching was evident for EmGFP that was dissolved in TAM_{15} buffer.

Determination of the fraction of active ribosomes

Cell-free protein expression was performed for 1 h at 30°C with 130 ng circular or linearized plasmid DNA per 10 µl reaction volume. Anti-tmRNA [SsrA (34)] at a final concentration of 5 µM (6) was premixed with the reaction mixture, and reaction was initiated with linearized plasmid. The reaction mixtures were incubated either in the plate reader while following fluorescence in real time, or in a temperature controlled bath for one hour and subsequently pulled-down through a sucrose cushion. In pull-down assays, reaction volumes of 30 µl were layered onto ice-cold 1.1 M sucrose in TAM_{15} buffer (100 µl) and centrifuged at 110 000 rpm for 40 min at 4°C. The supernatant was collected and the pellet was suspended in 30 µl TAM_{15} buffer. EmGFP in the supernatant and in the pellet were quantified in the plate reader using a fluorescence calibration curve (Supplementary Information 1 and Supplementary Figure S1). The calculated ratio of

EmGFP per ribosome in the pellet represented the fraction of active ribosomes.

[^{14}C]-Phe incorporation into EmGFP

Samples were prepared with CFPS^{-Phe} as described above, except the final sample volume was 15 µl. The [^{14}C]-Phe-tRNA^{Phe} variants were used at final concentrations of 10 µM. The reaction was initiated by plasmid addition and incubated at 30°C for 30 min. The reaction was quenched by the addition of 0.3 ml 5% TCA (ice-cold), heated to 95°C for 15 min, cooled on ice, filtered through a nitrocellulose filter, and washed five times with 1 ml of 5% ice-cold TCA. The filter was then dissolved in 1 ml ethyl acetate. Precipitated radioactivity, accurate to ±8%, was determined above a background equal to the radioactivity obtained with a sample that did not contain the EmGFP plasmid.

Fluorescence trace analysis

Four parameters were evaluated from the fluorescence traces that contained various Phe-tRNA^{Phe}s, using Origin software (OriginLab Corporation). Estimates of lag time, t_L, maximum synthesis rate, S_1 and final protein synthesis rate, S_2, were obtained from the time of the maximal value of the second derivative, the maximal value of the first derivative, and a linear fit of the last eleven time points, respectively. Amplitude of the rapid synthesis period, A_1, was determined by the intercept of two linear regression lines, the first centered at the point of maximal slope and the second fitted as described for S_2. Before taking derivatives, the traces were smoothed using a 5-point adjacent average. All linear fits were performed using 11 time points. All values were normalized to the data obtained for 2 µM *E. coli* Phe-tRNA^{Phe}.

Numerical simulations

A model of the kinetics of EmGFP fluorescence accumulation in the CFPS experiment was written in MATLAB version 7.5.0 (R2007b). Details of the algorithm are described in Supplementary Information. The MATLAB code is supplied as Supplementary File S2. A compiled executable file may also be obtained upon request to one of the corresponding authors.

RESULTS

Preliminary characterization of the cell-free coupled transcription/translation reaction

We employed a construct containing the 239-residue EmGFP sequence in between a 40-residue N-terminal His-tag extension and a 31-residue C-terminal extension. The latter sequence permitted the native EmGFP polypeptide to leave the ribosomal exit tunnel, allowing folding and maturation of EmGFP while the peptide is still attached to the ribosome. Translation of EmGFP followed by fluorophore maturation results in an accumulation of fluorescence intensity, providing a readily detectable signal that, after an initial lag phase, increases continuously in real time, reaching a near plateau after 60–90 min (Figure 1). Four different buffers were examined, with the amounts of fluorescent EmGFP formation falling in the order Polyamine (31) > TAM_{15} (11) > Polymix (30) ≫ TAM_7 (29) (Figure 1A), with the Polyamine buffer showing similar activity to the buffer provided with the kit (unknown composition). Accordingly, only the Polyamine buffer [having a composition similar to that used previously to support transcriptional activity (35)] or the TAM_{15} buffer was used in subsequent translational activity assays. We also tested whether pre-transcribed mRNA would program ribosomes to produce EmGFP in the CFPS kit. Translation rates and amounts were comparable to the coupled transcription-translation beginning from the DNA plasmid (data not shown).

We next determined the fraction of active ribosomes present in a CFPS kit, as measured by the amount of ribosome-associated nascent EmGFP complex formed, adapting a known procedure (26). In this approach the EmGFP plasmid is linearized to remove the stop codon, preventing re-initiation on a new mRNA, and anti-tmRNA oligonucleotide complementary to the tmRNA sequence is added to suppress the release of EmGFP from the stalled ribosome after translation of the last codon (6,36). The results (Table 1, Figure 1B) show higher total fluorescent EmGFP production for circular plasmid than for linearized plasmid, in accord with an earlier report (22). Addition of anti-tmRNA to the linearized plasmid further reduces EmGFP production. Here the slightly higher value of total mature EmGFP synthesized (0.36/ribosome) vs. mature EmGFP cosedimenting with ribosomes (0.29/ribosome) arises from some combination of incomplete suppression of EmGFP release (i.e. a small number of ribosomes expressing multiple EmGFPs) and/or dissociation of some ribosome-bound EmGFP during either the reaction or ultracentrifugation. The fraction of active ribosomes (0.29), as measured by co-sedimenting fluorescent EmGFP, provides an important benchmark for evaluating the quality of different preparations and/or batches of CFPS kits, and of exogenous ribosomes that are substituted for endogenous ribosomes (see below). For other batches of the CFPS kit this fraction varied from 0.18 to 0.33, which is in reasonable agreement with previously reported results for SecM-stalled ribosomes with a protein of similar length (6) and somewhat higher than found in a previous single molecule experiment using similar methods (26).

Table 1. Determination of fraction of active ribosome

Plasmid	Circular	Linear	Linear
Anti tmRNA	–	–	+
Total EmGFP/ribosome	1.62 ± 0.10	0.76 ± 0.05	0.36 ± 0.01
Co-sedimenting EmGFP/ ribosome	0.10 ± 0.01	0.05 ± 0.01	0.29 ± 0.01
Co-sedimenting EmGFP/total EmGFP	0.06 ± 0.01	0.06 ± 0.01	0.79 ± 0.02

All measurements were performed in triplicate and reported as means ± SD. EmGFP stoichiometry is estimated by fluorescence intensity, using the calibration curve shown in Supplementary Figure S1. Ribosome stoichiometry is estimated by 26 pmol/A_{260}.

Substitution of exogenous ribosomes for endogenous ribosomes

High speed centrifugation can be used to remove endogenous ribosomes from the CFPS kit, resulting in a preparation, denoted the CFPS$^{\text{-ribosome}}$ kit, that is inactive in the EmGFP expression assay, with activity restored by addition of exogenous ribosomes. We examined the restoration of activity as a function of the extent of ribosome purification (Figure 2A and 'Materials and Methods' section), using the circular EmGFP plasmid, and determined that minimal purification, consisting of ribosome pelleting by high-speed centrifugation of crude S30 lysate, gave the highest restored activity. Accordingly this preparation, denoted S100P ribosomes, was used in assays comparing the activities of several exogenously added ribosomes, including wild-type MRE600 ribosomes, AM77 ribosomes lacking protein L11 (37) and AM77 ribosomes reconstituted with either wild-type L11 (AM77$^{\text{L11}}$) or with an L11 variant labeled stoichiometrically at position 87 with Cy3 (AM77$^{\text{Cy3L11}}$) (11) (Figure 2B). These results, showing that the lower activity of the AM77 ribosomes is partially restored by reconstitution with either wild-type or Cy3-labeled L11, indicate that derivatization of L11 with Cy3 does not interfere with translational activity, in accord with earlier results measuring other ribosomal activities (9,38,39). Addition of initiation factors improves the activity of these exogenously added ribosome preparations (Supplementary information 2B and Supplementary Figure S3A and B).

For the CFPS kit used for the experiments shown in Figure 2B, 0.18 ± 0.02 of the endogenous ribosomes were active (determined as described above using the linearized EmGFP plasmid in the presence of anti-tmRNA), compared with 0.32 ± 0.05 of the exogenously added MRE600 ribosomes and 0.09 ± 0.01 and 0.10 ± 0.04, respectively, for exogenously added AM77 and AM77$^{\text{L11}}$ ribosomes. The lower fractions of active AM77-derived ribosomes account for the lower levels of EmGFP synthesis observed with these ribosomes (Figure 2B), although the intrinsic translation rate of active AM77-derived ribosomes is similar to that of wild-type ribosomes (see Supplementary Information 2A, and Supplementary Figure S2).

Substitution of exogenous for endogenous charged tRNAs

We next modified the EmGFP assay to permit comparison of the activities of added exogenous charged tRNA in supporting EmGFP expression. Below we detail our results with Phe-tRNA$^{\text{Phe}}$, although the approach is general and has also been applied successfully to Val-tRNA$^{\text{Val}}$ and Lys-tRNA$^{\text{Lys}}$. These experiments were performed using the circular EmGFP plasmid.

The principal challenge in the development of this modified assay was to prepare a CFPS$^{\text{-Phe}}$ kit (i.e. a kit depleted of all forms of Phe) such that synthesis of mature EmGFP was completely dependent on added exogenous Phe-tRNA$^{\text{Phe}}$ or Phe. This was accomplished by: (i) dialysis of the commercial CFPS lysate to remove all small molecules, including the amino acids; (ii) specific inhibition of Phe-amino-acyl tRNA synthetase (Phe-RS) with an active-site directed inhibitor; (iii) addition of a general protease inhibitor to prevent generation of Phe from protein breakdown; and (iv) adding back all of the small molecules required for protein synthesis with the exception of Phe (Supplementary Figure S3C). The ability of the resulting CFPS$^{\text{-Phe}}$ kit to produce detectable amounts of EmGFP was totally dependent on adding either exogenous yeast Phe-tRNA$^{\text{Phe}}$ (Figure 3A, Supplementary Figure S4A—similar results were obtained for *E. coli* Phe-tRNA$^{\text{Phe}}$; Supplementary Figure S4B) or Phe (Figure 3B) with maximal EmGFP expression requiring higher concentrations of Phe (80 μM) than of Phe-tRNA$^{\text{Phe}}$ (8–10 μM) (Figure 3C and D).

The curves of EmGFP fluorescence in Figure 3A and B can be characterized by four parameters, a lag phase corresponding to all dark events preceding EmGFP maturation (t_L), a region of high slope reflecting the maximum

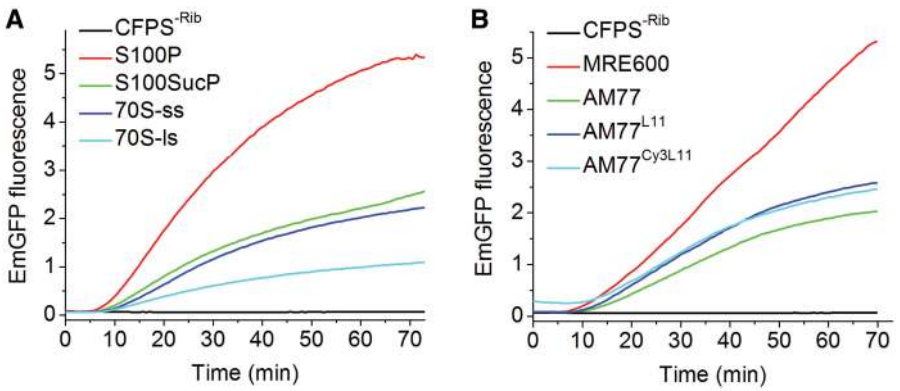

Figure 2. Cell-free expression of EmGFP on addition of exogenous ribosomes (1.5 μM) to the CFPS$^{\text{-ribosome}}$ kit. Experiments were performed with ribosome preparations dissolved in TAM$_{15}$ buffer mixed with CFPS reconstituted with the vendor-provided buffer, using the plate reader. (**A**) As a function of MRE600 ribosome purification: centrifugation of crude S30 lysate directly (S100P); through a sucrose cushion (S100sucP); small-scale (70S-ss) and large-scale (70S-ls) 70S purification via sucrose density-gradient centrifugation. A control ribosome-depleted sample (CFPS$^{\text{-Rib}}$) contained no added ribosomes. (**B**) S100P preparations of MRE600 and AM77 ribosomes. All samples contained the CFPS$^{\text{-ribosome}}$ kit. Due to the spectral overlap of Cy3 with EmGFP, the AM77$^{\text{Cy3L11}}$ trace exhibits slightly higher background. Experiments, repeated five times using different CFPS batches, gave reproducible results.

rate of fluorescent EmGFP formation (phase-1-slope, S_1), the total fluorescent EmGFP synthesized in the first, rapid phase of reaction (phase-1-amplitude, A_1), and a final region of lower slope (phase-2-slope, S_2) corresponding to a slower, second phase. Each of the latter three parameters shows a strong Phe-tRNA^{Phe} or Phe concentration dependence (Figure 3C and D, respectively). Both S_1 and A_1 increase nearly monotonically before reaching saturated values. S_2 increases monotonically over the limited range of Phe-tRNA^{Phe} concentrations employed, but goes through a maximum over the broader range of Phe concentration that was explored. In contrast, t_L has only minor dependence on either Phe-tRNA^{Phe} or Phe concentration. The overall maximal activities of the CFPS^{-Phe} kit with added Phe-tRNA^{Phe} (8-10 μM) or Phe (80 μM) were similar to one another (Supplementary Figure S3D), but reduced as compared with the unmodified CFPS kit, showing similar t_L values but 2- to 4-fold reductions in the values of S_1, S_2, and A_1 (Supplementary Table S1).

The CFPS^{-Phe} kit makes very efficient use of added Phe-tRNA^{Phe}. For a CFPS^{-Phe} kit containing a total active ribosome concentration of 0.6 μM, saturation of Phase-1-formation was reached by ~8 μM yeast Phe-tRNA^{Phe} (Figure 3C). As the encoded EmGFP has 14 Phe residues (2 in the N-terminal linker sequence and 12 in the original gene) the value of 8 μM of added Phe-tRNA^{Phe} found at saturation, in addition to the residual endogenous Phe-tRNA^{Phe} (2 μM) that we estimate to be present in the CFPS^{-Phe} kit (see below), is just slightly above the expected stoichiometric requirement of 8 μM Phe-tRNA^{Phe} needed to produce one EmGFP per active ribosome. This result indicates an apparent K_m for Phe-tRNA^{Phe} incorporation at cognate codons that is <1 μM, in accord with results derived from simpler model sytems (10,40,41). The apparent K_m for Phe, estimated from the concentration dependence of either S_1 or A_1, is ~10–15 μM. This value, which represents the first reported estimation of K_m for an amino acid in a CFPS system, is considerably higher than the value for Phe-RS (2 μM) determined in a highly purified system (42), perhaps reflecting competing binding to Phe-RS in the CFPS^{-Phe} kit by near cognate amino acids and/or added Phe-RS inhibitor.

Numerical simulations of multi-step EmGFP synthesis

We developed a numerical simulation of a reaction kinetics model in order to gain additional understanding about the effects of exogenous Phe-tRNA^{Phe} (see below) on the formation of EmGFP fluorescence using the CFPS^{-Phe} kit (Figure 3A). This model includes 315 steps, which proceed in series, and include: a transcription initiation step, a transcription elongation step, a translation initiation step, 310 translation elongation steps, utilizing 296

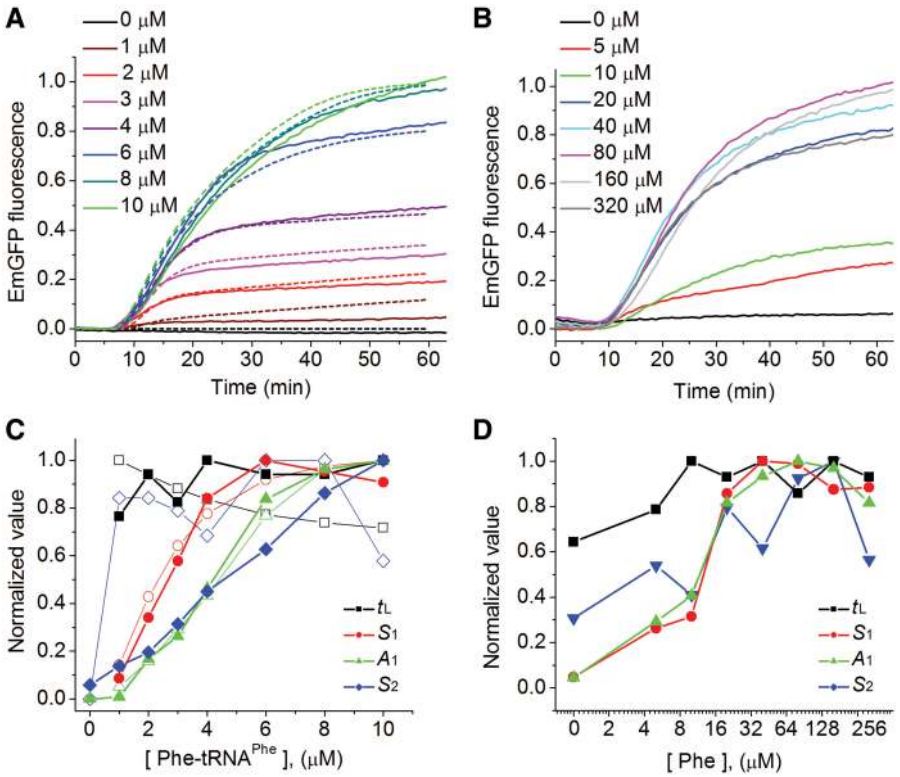

Figure 3. Cell-free expression of EmGFP using the CFPS^{-Phe} kit. Experiments were performed in Polyamine buffer, using the plate reader. (**A**) As a function of added [Phe-tRNA^{Phe}]. The dashed lines are derived from the numerical simulation model described in the text and in Supplementary Data. The active ribosome concentration was 0.58 ± 0.04 μM. Deviations from simulated values are attributable to various oversimplifications within the model, as well as to inhibitory effects expected at high concentrations of labeled deacylated tRNA^{Phe} (see Supplementary Data and Figure S3E). (**B**) As a function of added [Phe]. (**C** and **D**) Dependence of normalized parameters t_L, S_1, A_1 and S_2 (Table 2) on [Phe-tRNA^{Phe}] or [Phe], respectively. Solid symbols, measured values. Open symbols, values derived from the simulations of the various Phe-tRNA^{Phe} concentrations.

non-Phe aminoacyl-tRNAs and 14 Phe-tRNA^{Phe}s according to the EmGFP sequence, and two fluorophore maturation steps (35). Each non-Phe translation elongation step was assigned the same pseudo-first-order rate constant (k_1) and each Phe translation elongation step was assigned a second-order rate constant, k_2 for endogenous Phe-tRNA^{Phe} and k_2^* for exogenous Phe-tRNA^{Phe}. The pseudo-first-order rate process with rate constant k_1 reflects the large excess of each of the non-Phe aminoacyl-tRNAs present in the CFPS^{-Phe} kit while the second-order process, k_2, reflects the limited availability of the added Phe-tRNA^{Phe}.

In order to account for the rather small observed threshold value of exogenously added Phe-tRNA^{Phe} ($\sim$1 μM) that has to be exceeded in order to detect EmGFP fluorescence (Figure 3C), the model includes endogenous Phe-tRNA^{Phe} that is not completely removed in preparing the CFPS^{-Phe} kit and functionally heterogeneous ribosomes. If all of the ribosomes were equally active, small amounts of added Phe-tRNA^{Phe} would be consumed by synthesis of incomplete, non-fluorescent chains, leading to a considerably higher threshold Phe-tRNA^{Phe} concentration (Supplementary Figure S6). A final assumption is that protease and Phe-RS activities are incompletely inhibited in the CFPS^{-Phe} kit, allowing a continual slow regeneration of the limiting reagent, Phe-tRNA^{Phe}, that results in the slow second phase of EmGFP formation.

The kinetic model was used to simulate actual results obtained on adding varying Phe-tRNA^{Phe} concentrations to the CFPS^{-Phe} kit, as described below. Further details on the simulation may be found in Supplementary Information 4A.

Assaying the activity of labeled Phe-tRNA^{Phe} variants by EmGFP formation

We used the CFPS^{-Phe} kit to compare the relative activities of various Phe-tRNA^{Phe} variants in EmGFP synthesis. The Phe-tRNA^{Phe}s examined were *E. coli* and yeast, either unlabeled or labeled at dihydroU residues (16 and 17 in yeast or 16 and 20 in *E. coli* tRNA^{Phe}) to a total stoichiometry of 0.8 – 0.9 fluorophores/tRNA (Table 2) with either Cy3, Cy5, or Cy5.5 (10). Variants were examined at one to three concentrations over a concentration range, 1–4 μM (Figure 4A), for which both S_1 and A_1 are highly dependent on Phe-tRNA^{Phe} concentration (Figure 3C).

Although the simulation model described above adequately fits the data using identical values of k_2^* for both yeast and *E. coli* exogenous unlabeled Phe-tRNA^{Phe}s (equal to the k_2 value for endogenous Phe-tRNA^{Phe}), some variability in individual head-to-head comparisons caused slight differences in apparent activity, as is evident from Figure 4A. In contrast, the labeled Phe-tRNA^{Phe}s were consistently less active than the unlabeled Phe-tRNA^{Phe}s with respect to values of both S_1 and A_1 (Figure 4B and C, Table 2). A large increase in t_L is associated with the use of Cy5-labeled yeast Phe-tRNA^{Phe}, whereas t_L is not strongly affected by the other Phe-tRNA^{Phe}s. The relative activities of labeled Phe-tRNA^{Phe}s are reduced more strongly at higher concentrations (Table 2), suggesting that high concentrations of the labeled Phe-tRNA^{Phe} preparations are inhibitory. Such inhibition could be due, at least in part, to an increase in uncharged, labeled tRNAs in these preparations (Supplementary Figure S3E) that may offset the direct effect of raising Phe-tRNA^{Phe} concentration.

Table 2. Phe-tRNA^{Phe} variant parameters[a]

	E. coli	*E. coli* Cy3	*E. coli* Cy5	*E. coli* Cy5.5	Yeast	Yeast Cy3	Yeast Cy5
Phe-tRNA^{Phe} preparation (%)							
Labeling		80	90	79		92	93
Charging	28	25	15	26	44	37	30
Empirical parameters							
t_L[b] (2 μM)	1.00 ± 0.05	1.47 ± 0.11	1.13 ± 0.22	1.13 ± 0.08	1.20 ± 0.11	1.27 ± 0.11	2.33 ± 0.15
t_L[b] (4 μM)	1.27 ± 0.11	1.67 ± 0.04	1.07 ± 0.08	NA	1.07 ± 0.07	1.18 ± 0.11	2.27 ± 0.25
S_1[c] (2 μM)	1.00 ± 0.22	0.48 ± 0.17	0.42 ± 0.04	0.71 ± 0.19	0.79 ± 0.04	0.42 ± 0.02	0.21 ± 0.02
S_1[c] (4 μM)	2.34 ± 0.06	0.60 ± 0.07	0.43 ± 0.04	NA	1.43 ± 0.05	0.50 ± 0.03	0.09 ± 0.01
A_1[d] (2 μM)	1.00 ± 0.09	0.87 ± 0.10	0.35 ± 0.05	0.55 ± 0.17	1.02 ± 0.04	0.68 ± 0.01	0.38 ± 0.02
A_1[d] (4 μM)	2.89 ± 0.06	1.52 ± 0.09	0.81 ± 0.03	NA	2.41 ± 0.01	1.24 ± 0.06	0.50 ± 0.02
S_2[e] (2 μM)	1.00 ± 0.14	1.17 ± 0.15	0.63 ± 0.07	0.37 ± 0.18	1.14 ± 0.08	0.71 ± 0.09	0.68 ± 0.04
S_2[e] (4 μM)	2.61 ± 0.12	1.54 ± 0.12	0.78 ± 0.11	NA ±	1.74 ± 0.03	1.03 ± 0.05	0.73 ± 0.09
Relative ^{14}C-Phe incorporation[f]	1.00 ± 0.02	0.98 ± 0.02	0.13 ± 0.01	NA	0.66 ± 0.01	0.43 ± 0.02	0.12 ± 0.01
Simulation							
Relative k_2^*	1[g]	0.1	0.025	0.2	1[g]	0.05	0.025
Phase 2 steady-state Phe-tRNA^{Phe} concentration (μM)	0.1	0.1	0.01	0.01	0.15	0.025	0

[a]Data at 2 μM added Phe-tRNA^{Phe} are presented in Figure 4B and C. Parallel results obtained at 4 μM Phe-tRNA^{Phe} are summarized in the table. Experiments were performed using 2–5 repeats. Data obtained with 2 μM *E. coli* tRNA variants was repeated with two different CFPS batches. All values were normalized to 2 μM *E. coli* Phe-tRNA^{Phe}.
[b]Lag time.
[c]Phase-1-slope.
[d]Phase-1-amplitude.
[e]Phase-2-slope.
[f]After 30-min incubation.
[g]Equal to k_2.

Because of the apparent inhibition at high labeled Phe-tRNA^{Phe} concentrations, only the time-courses of fluorescent EmGFP formation using 2 μM exogenous labeled Phe-tRNA^{Phe} (Figure 4B and C) were fit with the kinetic simulation model. The resulting k_2^* values (Table 2) show that the activities of the labeled tRNAs, relative to *E. coli* Phe-tRNA^{Phe}, fall in the order Cy5.5 (5-fold reduction) > Cy3 (10-fold reduction) > Cy5 (40–fold reduction). The order of activity found with these dyes suggests that activity loss results from a combination of steric bulk and hydrophobicity, since Cy3 is both smaller and less hydrophobic than Cy5, whereas Cy5.5, a dianion at neutral pH, is both larger and less hydrophobic than Cy5.

Assaying the activity of Phe-tRNA^{Phe} variants by [^{14}C]-Phe incorporation

Plasmid-dependent [^{14}C]-Phe incorporation into polypeptide during EmGFP synthesis provides an alternative measure of the relative activities of labeled Phe-tRNA^{Phe} in protein synthesis. [^{14}C]-Phe incorporation is less stringent than the EmGFP fluorescence assay, since it measures synthesis of partial and full-length EmGFP chains regardless of correct folding or chromophore maturation. Indeed, for the results presented in Table 2 using unlabeled *E. coli* or yeast Phe-tRNA^{Phe}, only 35–40% of the [^{14}C]-Phe incorporated into precipitable peptide chains was incorporated in full-length fluorescent EmGFP protein in the first 30 min of the reaction, as determined by carrying out both analyses on the same sample. The relative [^{14}C]-Phe incorporation levels are consistent with relative activities observed in ensemble measurements of polyPhe synthesis and single molecule translation of short stretches of model mRNAs using these same labeled tRNAs (10,11). Qualitatively, the relative [^{14}C]-Phe incorporation levels showing Phe-tRNA^{Phe} (Cy3) to be more active than Phe-tRNA^{Phe} (Cy5) for both *E. coli* and yeast tRNAs parallel the order of relative activities found in the fluorescence assay measured either by k_2^* or A_1 values (Table 2).

DISCUSSION

Here we describe a convenient, fluorescence-based assay that, via adaptation of a commercially available bacterial CFPS kit, permits quantitative determination of the effects on the rate and stoichiometry of fluorescent EmGFP expression of replacing endogenous with exogenous components of the protein synthesis machinery. An important adjunct to this assay is the quantification of the fraction of active ribosomes in either the CFPS kit itself, or in a sample from which endogenous ribosomes have been removed (the CFPS$^{-ribosome}$ kit) and replaced. Approximately 20–30% of the ribosomes in the commercial CFPS kit are active in fluorescent EmGFP expression. By comparison, wild-type MRE600 ribosomes prepared by us show ~30% activity, whereas the fractional activities of the mutant AM77 ribosomes which lack protein L11, even when supplemented with L11, are distinctly lower (~10%).

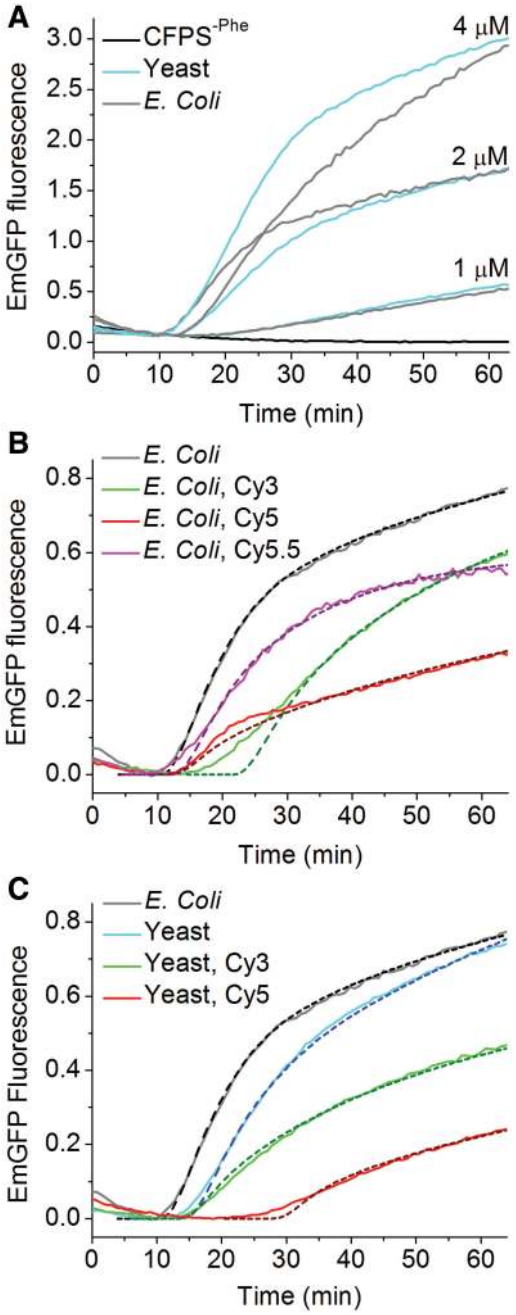

Figure 4. Comparisons of cell-free expression of EmGFP on addition of Phe-tRNA^{Phe} variants to the CFPS^{-Phe} kit. EmGFP fluorescence measurements contained an active ribosome concentration of 0.30 ± 0.02 μM. (**A**) Various concentrations of unlabeled *E. coli* and yeast Phe-tRNA^{Phe}. (**B**) *Escherichia coli* variants (2 μM). (**C**) Yeast variants (2 μM). Unlabeled *E. coli* Phe-tRNA^{Phe} is included in each panel for ease of comparison. The dashed lines are derived from the numerical simulation model using the parameter values listed in Table 2 and given in the text.

As described above, replacement of endogenous ribosomes is quite facile, since exogenous ribosomes prepared directly from crude cell extracts ('S100P' ribosomes) confer the highest activity when added to the easily prepared CFPS$^{-ribosome}$ kit. Replacement of endogenous

Phe-tRNA^{Phe} is somewhat more demanding, but relatively straightforward using the optimized procedures detailed in 'Materials and Methods' section. In order to selectively remove Phe-tRNA^{Phe}, we elected to prepare a CFPS^{-Phe} kit in which the endogenous tRNA^{Phe} is retained, but Phe is depleted and Phe-RS is inhibited. With the CFPS^{-Phe} kit, fluorescent EmGFP expression is totally dependent on either added Phe (Figure 3B) or added Phe-tRNA^{Phe}, at much lower concentration (Figure 3A). An alternative approach for preparing a CFPS^{-Phe} system, which we are currently pursuing, utilizes PURExpress® (New England Biolabs), a cell-free transcription/translation system reconstituted from purified *E. coli* components, including each of the tRNA synthetase enzymes (43). A custom-made PURExpress® mixture should essentially eliminate the residual Phe-tRNA^{Phe} and Phe-RS content present in a CFPS^{-Phe} kit.

Our primary goal in developing adaptations of CFPS kit assay for the expression of fluorescent EmGFP was to permit determination of the effects on translational activity of fluorescent labeling of components of the protein synthesis machinery, in particular ribosomes and tRNAs, since such labeling is used extensively in both ensemble and single molecule studies of the mechanism of protein synthesis (12–15). The results showing that dye-labeled Phe-tRNA^{Phe}s have substantially lower activity than unlabeled Phe-tRNA^{Phe} in supporting full-length protein synthesis highlight the need to explore alternative labeling strategies to produce labeled tRNAs with higher intrinsic activities. Such strategies could include using tRNA transcripts so as to be able to direct labeling to a unique DHU position (44) as opposed to native tRNAs, for which labeling is distributed over all DHU positions (45,46); using less hydrophobic fluorophores; and introducing fluorophores at other than DHU positions (47–49).

In addition to meeting our primary goal, continuous monitoring of the formation of fluorescent EmGFP by simple or modified CFPS kits provides a general, radioactivity-free approach, amenable to high-throughput screening, for evaluating effects on the efficiency of protein synthesis of various additions, subtractions or substitutions to the protein synthesis machinery. These include (i) any kind of tRNA, rRNA or ribosomal protein variation, including mutation or enzymatic or chemical modification; (ii) addition of agents affecting transcription, translation, or protein folding (e.g. antibiotic screening effects on translation could be separated from those on transcription by initiating EmGFP synthesis with added mRNA, transcribed separately, rather than with added DNA); (iii) substituting amino acid analogues for native amino acids, whether measured by supplementing a CFPS$^{-aminoacid}$ kit with the amino acid analogue or with a tRNA charged with the analogue (50). In some experiments, suitable controls would be needed to exclude possible artifacts due to direct effects on EmGFP fluorescence. Finally, a CFPS$^{-aminoacid}$ kit, reconstituted with an isotopically labeled amino acid, could be used to prepare isotopically labeled proteins for IR and NMR studies.

SUPPLEMENTARY DATA

Supplementary Data are available at NAR Online: Supplementary Tables S1–S3, Supplementary Figures S1–S6, Supplementary Information Files S1–S2 and Supplementary Reference [51].

ACKNOWLEDGEMENTS

We thank Dr Olga Lozynska in Professor Scott Diamond's group at Penn for her help with the plate reader.

FUNDING

National Institutes of Health (GM080376 to B.S.C., Y.E.G.); Human Frontier Science Program fellowship (to G.R.). Funding for open access charge: National Institutes of Health (GM080376).

Conflict of interest statement. Y.E.G. and B.S.C. are paid consultants for Anima Cell Metrology.

REFERENCES

1. Zubay,G. (1973) In vitro synthesis of protein in microbial systems. *Annu. Rev. Genet.*, **7**, 267–287.
2. Schwarz,D., Junge,F., Durst,F., Frölich,N., Schneider,B., Reckel,S., Sobhanifar,S., Dötsch,V. and Bernhard,F. (2007) Preparative scale expression of membrane proteins in Escherichia coli-based continuous exchange cell-free systems. *Nat. Protoc*, **2**, 2945–2957.
3. Langer,M., Rothe,M., Eck,J., Mockel,B. and Zinke,H. (1996) A nonradioactive assay for ribosome-inactivating proteins. *Anal. Biochem.*, **243**, 150–153.
4. Brandi,L., Fabbretti,A., Milon,P., Carotti,M., Pon,C.L. and Gualerzi,C.O. (2007) Methods for identifying compounds that specifically target translation. *Meth. Enzymol.*, **431**, 229–267.
5. Jefferson,E.A., Arakawa,S., Blyn,L.B., Miyaji,A., Osgood,S.A., Ranken,R., Risen,L.M. and Swayze,E.E. (2002) New inhibitors of bacterial protein synthesis from a combinatorial library of macrocycles. *J. Med. Chem.*, **45**, 3430–3439.
6. Evans,M.S., Ugrinov,K.G., Frese,M.A. and Clark,P.L. (2005) Homogeneous stalled ribosome nascent chain complexes produced in vivo or in vitro. *Nat. Methods*, **2**, 757–762.
7. Underwood,K.A., Swartz,J.R. and Puglisi,J.D. (2005) Quantitative polysome analysis identifies limitations in bacterial cell-free protein synthesis. *Biotechnol. Bioeng.*, **91**, 425–435.
8. Liu,H., Pan,D., Pech,M. and Cooperman,B.S. (2011) Interrupted catalysis: the EF4 (LepA) effect on back-translocation. *J. Mol. Biol.*, **396**, 1043–1052.
9. Qin,H., Grigoriadou,C. and Cooperman,B.S. (2009) Interaction of IF2 with the ribosomal GTPase-associated center during 70S initiation complex formation. *Biochemistry*, **48**, 4699–4706.
10. Pan,D., Qin,H. and Cooperman,B.S. (2009) Synthesis and functional activity of tRNAs labeled with fluorescent hydrazides in the D-loop. *RNA*, **15**, 346–354.
11. Chen,C., Stevens,B., Kaur,J., Cabral,D., Liu,H., Wang,Y., Zhang,H., Rosenblum,G., Smilansky,Z., Goldman,Y.E. *et al.* (2011) Single-molecule fluorescence measurements of ribosomal translocation dynamics. *Mol. Cell*, **42**, 367–377.
12. Blanchard,S.C. (2009) Single-molecule observations of ribosome function. *Curr. Opin. Struct. Biol.*, **19**, 103–109.
13. Frank,J. and Gonzalez,R.L. Jr (2010) Structure and dynamics of a processive Brownian motor: the translating ribosome. *Annu. Rev. Biochem.*, **79**, 381–412.
14. Korostelev,A., Ermolenko,D.N. and Noller,H.F. (2008) Structural dynamics of the ribosome. *Curr. Opin. Chem. Biol.*, **12**, 674–683.

15. Petrov,A., Kornberg,G., O'Leary,S., Tsai,A., Uemura,S. and Puglisi,J.D. (2011) Dynamics of the translational machinery. *Curr. Opin. Struct. Biol.*, **21**, 137–145.
16. Iskakova,M.B., Szaflarski,W., Dreyfus,M., Remme,J. and Nierhaus,K.H. (2006) Troubleshooting coupled in vitro transcription-translation system derived from Escherichia coli cells: synthesis of high-yield fully active proteins. *Nucleic Acids Res.*, **34**, e135.
17. Mureev,S., Kovtun,O., Nguyen,U.T. and Alexandrov,K. (2009) Species-independent translational leaders facilitate cell-free expression. *Nat. Biotechnol.*, **27**, 747–752.
18. Zubay,G., Lederman,M. and DeVries,J.K. (1967) DNA-directed peptide synthesis. 3. Repression of beta-galactosidase synthesis and inhibition of repressor by inducer in a cell-free system. *Proc. Natl Acad. Sci. USA*, **58**, 1669–1675.
19. Kim,D.M. and Swartz,J.R. (2001) Regeneration of adenosine triphosphate from glycolytic intermediates for cell-free protein synthesis. *Biotechnol. Bioeng.*, **74**, 309–316.
20. DeVries,J.K. and Zubay,G. (1967) DNA-directed peptide synthesis. II. The synthesis of the alpha-fragment of the enzyme beta-galactosidase. *Proc. Natl Acad. Sci. USA*, **57**, 1010–1012.
21. Jelenc,P.C. and Kurland,C.G. (1979) Nucleoside triphosphate regeneration decreases the frequency of translation errors. *Proc. Natl Acad. Sci. USA*, **76**, 3174–3178.
22. Kudlicki,W., Kramer,G. and Hardesty,B. (1992) High efficiency cell-free synthesis of proteins: refinement of the coupled transcription/translation system. *Anal. Biochem.*, **206**, 389–393.
23. Tsien,R.Y. (1998) The green fluorescent protein. *Ann. Rev. Biochem.*, **67**, 509–544.
24. Hoffmann,M., Nemetz,C., Madin,K. and Buchberger,B. (2004) Rapid translation system: a novel cell-free way from gene to protein. *Biotechnol. Annu. Rev.*, **10**, 1–30.
25. Cooperman,B.S., Jaynes,E.N., Brunswick,D.J. and Luddy,M.A. (1975) Photoincorporation of puromycin and N-(ethyl-2-diazomalonyl)puromycin into Escherichia coli ribosomes. *Proc. Natl Acad. Sci. USA*, **72**, 2974–2978.
26. Katranidis,A., Atta,D., Schlesinger,R., Nierhaus,K.H., Choli-Papadopoulou,T., Gregor,I., Gerrits,M., Büldt,G. and Fitter,J. (2009) Fast biosynthesis of GFP molecules: a single-molecule fluorescence study. *Angew. Chem. Int. Ed. Engl.*, **48**, 1758–1761.
27. Rodnina,M.V. and Wintermeyer,W. (1995) GTP consumption of elongation factor Tu during translation of heteropolymeric mRNAs. *Proc. Natl Acad Sci USA*, **92**, 1945–1949.
28. Olah,T.V., Olson,H.M., Glitz,D.G. and Cooperman,B.S. (1988) Incorporation of single dinitrophenyl-modified proteins into the 30 S subunit of Escherichia coli ribosomes by total reconstitution. *J. Biol. Chem.*, **263**, 4795–4800.
29. Semenkov,Y.P., Rodnina,M.V. and Wintermeyer,W. (1996) The "allosteric three-site model" of elongation cannot be confirmed in a well-defined ribosome system from Escherichia coli. *Proc. Natl Acad Sci. USA*, **93**, 12183–12188.
30. Fei,J., Kosuri,P., MacDougall,D.D. and Gonzalez,R.L. Jr (2008) Coupling of ribosomal L1 stalk and tRNA dynamics during translation elongation. *Mol. Cell*, **30**, 348–359.
31. Dinos,G., Kalpaxis,D.L., Wilson,D.N. and Nierhaus,K.H. (2005) Deacylated tRNA is released from the E site upon A site occupation but before GTP is hydrolyzed by EF-Tu. *Nucleic Acids Res.*, **33**, 5291–5296.
32. Santi,D.V., Cunnion,S.O., Anderson,R.T. and Webster,R.W. Jr (1979) In vivo inhibitors of Escherichia coli phenylalanyl-tRNA synthetase. *J. Med. Chem.*, **22**, 1260–1263.
33. Shaner,N.C., Steinbach,P.A. and Tsien,R.Y. (2005) A guide to choosing fluorescent proteins. *Nat. Methods*, **2**, 905–909.
34. Tu,G.F., Reid,G.E., Zhang,J.G., Moritz,R.L. and Simpson,R.J. (1995) C-terminal extension of truncated recombinant proteins in Escherichia coli with a 10Sa RNA decapeptide. *J. Biol. Chem.*, **270**, 9322–9326.
35. Gilmore,R., Collins,P., Johnson,J., Kellaris,K. and Rapiejko,P. (1991) Transcription of full-length and truncated mRNA transcripts to study protein translocation across the endoplasmic reticulum. *Methods Cell Biol.*, **34**, 223–239.
36. Hanes,J. and Pluckthun,A. (1997) In vitro selection and evolution of functional proteins by using ribosome display. *Proc. Natl Acad Sci. USA*, **94**, 4937–4942.
37. Dabbs,E.R. (1979) Selection for Escherichia coli mutants with proteins missing from the ribosome. *J. Bacteriol.*, **140**, 734–737.
38. Seo,H.S., Abedin,S., Kamp,D., Wilson,D.N., Nierhaus,K.H. and Cooperman,B.S. (2006) EF-G-dependent GTPase on the ribosome. conformational change and fusidic acid inhibition. *Biochemistry*, **45**, 2504–2514.
39. Wang,Y., Qin,H., Kudaravalli,R.D., Kirillov,S.V., Dempsey,G.T., Pan,D., Cooperman,B.S. and Goldman,Y.E. (2007) Single-molecule structural dynamics of EF-G–ribosome interaction during translocation. *Biochemistry*, **46**, 10767–10775.
40. Gromadski,K.B. and Rodnina,M.V. (2004) Kinetic determinants of high-fidelity tRNA discrimination on the ribosome. *Mol. Cell*, **13**, 191–200.
41. Uemura,S., Aitken,C.E., Korlach,J., Flusberg,B.A., Turner,S.W. and Puglisi,J.D. (2010) Real-time tRNA transit on single translating ribosomes at codon resolution. *Nature*, **464**, 1012–1017.
42. Gabius,H.J., von der Haar,F. and Cramer,F. (1983) Evolutionary aspects of accuracy of phenylalanyl-tRNA synthetase. A comparative study with enzymes from Escherichia coli, Saccharomyces cerevisiae, Neurospora crassa, and turkey liver using phenylalanine analogues. *Biochemistry*, **22**, 2331–2339.
43. Shimizu,Y., Inoue,A., Tomari,Y., Suzuki,T., Yokogawa,T., Nishikawa,K. and Ueda,T. (2001) Cell-free translation reconstituted with purified components. *Nat. Biotechnol.*, **19**, 751–755.
44. Betteridge,T., Liu,H., Gamper,H., Kirillov,S., Cooperman,B.S. and Hou,Y.M. (2007) Fluorescent labeling of tRNAs for dynamics experiments. *RNA*, **13**, 1594–1601.
45. Kaur,J., Raj,M. and Cooperman,B.S. (2011) Fluorescent labeling of tRNA dihydrouridine residues: Mechanism and distribution. *RNA*, **17**, 1393–1400.
46. Wintermeyer,W. and Zachau,H.G. (1979) Fluorescent derivatives of yeast tRNAPhe. *Eur. J. Biochem.*, **98**, 465–475.
47. Haller,A., Souliére,M.F. and Micura,R. (2011) The dynamic nature of RNA as key to understanding riboswitch mechanisms. *Acc. Chem. Res.*, **44**, 1339–1348.
48. Motorin,Y., Burhenne,J., Teimer,R., Koynov,K., Willnow,S., Weinhold,E. and Helm,M. (2011) Expanding the chemical scope of RNA:methyltransferases to site-specific alkynylation of RNA for click labeling. *Nucleic Acids Res.*, **39**, 1943–1952.
49. Paige,J.S., Wu,K.Y. and Jaffrey,S.R. (2011) RNA mimics of green fluorescent protein. *Science*, **333**, 642–646.
50. Murakami,H., Saito,H. and Suga,H. (2003) A versatile tRNA aminoacylation catalyst based on RNA. *Chem. Biol.*, **10**, 655–662.
51. Teerawanichpan,P., Hoffman,T., Ashe,P., Datla,R. and Selvaraj,G. (2007) Investigations of combinations of mutations in the jellyfish green fluorescent protein (GFP) that afford brighter fluorescence, and use of a version (VisGreen) in plant, bacterial, and animal cells. *Biochim. Biophys. Acta*, **1770**, 1360–1368.